Available at www.sciencedirect.com

ScienceDirect

journal homepage: www.elsevier.com/locate/watres

Characterisation of initial fouling in aerobic submerged membrane bioreactors in relation to physico-chemical characteristics under different flux conditions

*Tze Chiang Albert Ng, How Yong Ng**

Division of Environmental Science and Engineering, National University of Singapore, 9 Engineering Drive 1, EA-03-12, Singapore 117576, Singapore

ARTICLE INFO

Article history:
Received 22 April 2009
Received in revised form
16 November 2009
Accepted 22 December 2009
Available online 6 January 2010

Keywords:
Confocal laser scanning microscope (CLSM)
Excitation–emission matrix (EEM)
Extracellular polymeric substances (EPS)
Submerged membrane bioreactor (sMBR)
Soluble microbial products (SMP)

ABSTRACT

The initial fouling characteristics of aerobic submerged membrane bioreactors (MBRs) were analysed under different flux conditions. Physico-chemical analyses of the mixed liquor hinted that carbohydrates were more important to membrane fouling than proteins. However, this contrasted with the characterisation of foulants on the membrane surfaces. Micro-structural analyses of the foulants on the membrane surfaces showed that the dominant foulants were different under different flux conditions. Membrane fouling occurred through a biofilm-dominated process under lower flux conditions, but the mechanism shifted towards a non-biofilm, organic fouling process as the flux was increased. In spite of the differences in fouling mechanisms, it was found that the protein fraction on the membrane surfaces, in the initial stages of MBR operations, had the greatest impact in the rise of transmembrane pressure.

1. Introduction

Membrane bioreactor (MBR) is a system that combines biological treatment with a membrane for physical filtration to separate the liquid component from the mixed liquor. A cross-flow MBR provides a membrane module outside of the biological treatment tank while a submerged MBR (sMBR) merges both processes into a single unit. The MBR system is gaining much popularity in treatment of wastewater due to its efficacy in producing high quality effluent by providing complete solid–liquid separation regardless of fluctuations in the influent quality (Visvanathan et al., 2000), with the sMBR being more popular because of its lower energy requirements (Gander et al. 2000). However, operational challenges leading to increased costs, particularly the inevitable membrane fouling, have limited wide-scale adoption of this technology. Membrane fouling, caused by a deposition of substances on the membrane surface and/or within membrane pores results in performance deterioration with either a decrease in permeate flux, or an increase in transmembrane pressure (TMP).

Many studies have been conducted to elucidate the effect of various factors on membrane fouling. Other than the intrinsic properties of the membrane material, these factors

* *Corresponding author*. Tel.: +65 65164777; fax: +65 67744202.
E-mail address: esenghy@nus.edu.sg (H.Y. Ng).
0043-1354/$ – see front matter © 2010 Elsevier Ltd. All rights reserved.
doi:10.1016/j.watres.2009.12.038

Nomenclature

a	specific filtration resistance (kg^{-1} m)
A	membrane surface area (m^2)
C_b	concentration of bulk solution (kg m^{-3})
CLSM	confocal laser scanning microscopy
d_p	particle diameter (m)
DO	dissolved oxygen
EEM	excitation-emission matrix
EPS	extracellular polymeric substances
HRT	hydraulic retention time (h)
J	flux (L m^{-2} h^{-1})
MBR	membrane bioreactor
R_g	hydrodynamic resistance of gel layer (m^{-1})
R_m	resistance of membrane (m^{-1})
MLSS	mixed liquor suspended solids (g L^{-1})
sMBR	submerged MBR
SMP	soluble microbial products
SRT	solids retention time (d)
TMP	transmembrane pressure (Pa)
V	filtrate volume (m^3)
ε	porosity
η	viscosity (N s^{-1} m^{-2})
ρ	density (kg m^{-3})

can be categorised into two main groups, namely operational- and sludge-related factors. Operational-related factors, such as operating flux, solids retention time (SRT), loading rate, dissolved oxygen concentration and so on, affect membrane fouling either directly or indirectly by altering biomass characteristics (Chang and Judd, 2002; Psoch and Schiewer, 2006; Jang et al., 2007). Biomass characteristics include sludge viscosity (Meng et al., 2006), mixed liquor suspended solids (MLSS) concentration (Chang and Kim, 2005), soluble microbial products (SMP) and extracellular polymeric substances (EPS) concentrations (Jeong et al., 2007), and microbial community (Ma et al., 2006). An MBR with a higher DO concentration results in better filterability and a lower fouling rate. This has been attributed to the decreases in small biomass flocs and in cake resistance (Kang et al., 2003; Jin et al., 2006; Kim et al., 2006). Low SRT increases fouling tendency in MBRs due to higher SMP concentrations (Ng et al., 2006; Liang et al., 2007) and lower EPS concentrations (Nuengjamnong et al., 2005). However, due to the many interrelated parameters, conflicting results have been attained by different research groups. Since fouling of polymeric membranes is typically a result of interaction between polymeric surfaces and mixed liquor, biomass characteristics play a major role in membrane fouling (Kang et al., 2002). Therefore, a study on the effect of MLSS, EPS, and SMP concentrations on membrane fouling in tandem to the foulants found on the membrane surface under different flux conditions is highly desirable for the application of MBR to wastewater treatment at higher flux operations than currently possible.

In addition, the mechanism of membrane fouling may be better studied in terms of the micro-structural characteristics of the fouling layer. It is widely known that the formation of an organic layer during initial stages of membrane filtration leads to subsequent fouling layer development on the membrane surface. And the presence of these layers on the membrane surfaces is a major factor causing increase in the TMP. For biofilm fouling, structures of biofilm are highly variable, ranging from discontinuous colonies to thick continuous biofilms (Lewandowski, 2004). A better understanding of the different nature of the structure of the fouling layer in relation to the operating flux may explain the effects other parameters have on membrane fouling. A comparison of the micro-structural characteristics with TMP may help expound the effects individual constituents have on membrane fouling.

The aim of this study was to understand the effects of different constituents in the fouling layer have on TMP and to determine which parameter is important in the initial fouling of the membrane surface. For these objectives, the organic fouling layer on the membrane surface at prescribed times of operation were section and stained with different stains and confocal laser scanning microscopy (CLSM) images were obtained. The parameters describing structural characteristics of the fouling layer were then calculated from the CLSM images obtained using the Image Structural Analysis (ISA-2) software (Beyenal et al., 2004a) and compared to one another to describe the fouling layer under different flux conditions.

2. Materials and methods

2.1. MBR set-up

Three identical MBRs were operated simultaneously in this study to prevent different in operations due to temporal fluctuations (Fig. 1). Two flat-sheet polyolefin membranes with a nominal pore size of 0.45 μm, attached to a single module support, were immersed into each MBR. The effective

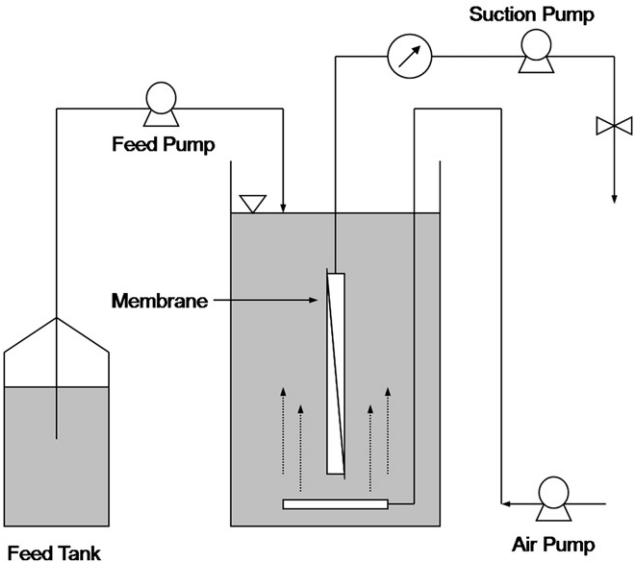

Fig. 1 – MBR schematic.

Table 1 – MBR operating conditions.

	Sub-critical	Critical	Super-critical
Working volume (L)	7	7	7
DO concentration (mg/L)	4.0 ± 0.5	4.0 ± 0.5	4.0 ± 0.5
pH	7.1 ± 0.2	7.1 ± 0.2	7.1 ± 0.2
Initial MLSS concentration (g/L)	7.5 ± 0.5	7.5 ± 0.5	7.5 ± 0.5
Average MLSS concentration (g/L)	7.5 ± 0.5	11.2 ± 2.8	11.9 ± 2.7
SRT (d)	20	20	20
Flux (LMH)	13.6	49.1	81.8
HRT (h)	5.8	1.6	1.0
Suction cycle	8-min suction; 2-min rest	8-min suction; 2-min rest	8-min suction; 2-min rest

area of the membrane was 0.11 m^2, and the contact angle of the clean membrane surface was found to be 72°. In order to minimise effects from variations in feed conditions, synthetic wastewater was supplied continuously to the MBRs. The synthetic wastewater composed of 470 mg L^{-1} glucose, 180 mg L^{-1} sodium bicarbonate, 96 mg L^{-1} ammonium chloride, 28 mg L^{-1} potassium phosphate, 14 mg L^{-1} ferric chloride, 5 mg L^{-1} magnesium chloride, 5 mg L^{-1} calcium chloride, 4 mg L^{-1} cobalt chloride, and 1 mg L^{-1} sodium molybdate.

The MBRs were initially operated for 8 weeks for sludge acclimatisation before experiments on the fouling mechanism commenced. During acclimatisation, the DO concentration was maintained at 4.0 ± 0.5 mg L^{-1}, and the pH controlled at 7.2 ± 0.2. Permeate flux was initially controlled at 14 L m^{-2} h^{-1}, with an intermittent suction cycle of 8-min run and 2-min pause carried out for permeate production. Hydraulic retention time (HRT) was initially set at 6 h and the SRT was set at 20 d. Operating conditions of the sludge acclimatisation stage were continued in one of the MBRs, which was to be operated at sub-critical flux conditions. The other two MBRs were operated at critical and super-critical flux conditions. The three MBRs operated at sub-critical flux, critical flux, and super-critical flux conditions are denoted as MBR_{sub}, MBR_{crit}, and MBR_{sup}, respectively. The HRT and operating flux of MBR_{crit} were 1.5 h and 49 L m^{-2} h^{-1}, respectively, while MBR_{sup} had an HRT of 1 h and an operating flux of 82 L m^{-2} h^{-1}. All other operating parameters remained the same. A summary of the operating conditions is shown in Table 1.

New membranes were immersed into the MBRs immediately after acclimatisation. Individual MBR was shut down after its TMP reached a value of 30 kPa. Each MBR was re-acclimatised for 30 d under conditions similar to the acclimatisation stage described earlier before a repeat of the fouling study was conducted. Three identical sets of experiments, with chemical cleaning of the membranes between each set before being re-submerged into the MBRs, were carried out in this research study for statistical confidence.

2.2. Physico-chemical analyses

MLSS concentrations were measured in accordance to the analytical methods described in the Standard Methods for Water and Wastewater (APHA, 2005). SMP was obtained first by centrifuging biomass samples at 9000 rpm for 10 min at 4 °C, then by filtering the supernatant though a 0.45-μm cellulose acetate membrane (GN-6 grid 47-mm, Gelman Science). To extract EPS, an equivalent volume of MilliQ water was added to the remaining sludge pellet. The mixture was vortexed vigorously for 10 min before placing in a heated water bath at 80 °C for 10 min. The sample was immediately centrifuged at 9000 rpm, 4 °C for 10 min. The supernatant was then filtered again through a 0.45-μm cellulose acetate membrane. The filtrate collected was the EPS sample used in the study. Protein and carbohydrate concentrations in the SMP and EPS samples were measured by the Lowry method (Lowry et al., 1951) and the phenol-sulphuric method (Dubois et al., 1956), respectively. Standards used for protein and carbohydrates concentration measurement were bovine serum albumin and glucose, respectively.

Excitation-emission matrix (EEM) fluorescence spectroscopy was conducted on the permeate, SMP, and EPS samples collected at the end of each experimental run. This technique is able to distinguish the compounds in the samples since peaks in an EEM are associated with the compounds' functional group (Kimura et al., 2009). For example, tryptophan-, microbial by-product-, humic- and fluvic-like compounds have been shown to occupy different regions in the EEM plot (Chen et al., 2003). A fluorescence spectrophotometer (LS 55, Perkin Elmer Co.) was used for obtaining the EEM spectra. Emission spectra between the wavelengths of 230 and 550 nm were collected at 0.5-nm increments by varying the excitation wavelength from 230 to 550 nm at 5-nm intervals. Excitation and emission slits were set at 10 nm with a scanning speed of 1000 nm min^{-1}.

2.3. Membrane sampling design

Membrane sampling was conducted at pre-defined times of 1st, 6th, 24th h of operation and subsequently at an interval of 24 h. Tests on the membrane samples were performed immediately and completed within 24 h from the sampling time.

Due to the use of an air diffuser to provide aeration and membrane scouring, there was a possibility for the air bubbles to lose their scouring efficacy along the height of the membrane. This may lead to possible fouling stratification, in which the lower half of the membrane module is less fouled than that of the top half. In order to eliminate effects of possible fouling stratification along the module within each MBR, random samples were taken from the two sections (top and bottom halves) of the membrane and analysed for their fouling constituents and structural characteristics. Membrane

samples of the other operated MBRs were obtained from the same locations as well.

Since microscopy work is typically subjected to operators' bias, to negate this form of bias, fifteen pre-determined positions on each membrane sample were used for CLSM imaging. All the identically-sized membrane samples were subjected to the same imaging positions and conditions before structural analyses were conducted on the images obtained.

2.4. *Confocal laser scanning microscopy*

The membrane samples containing the organic fouling layer were stained as described in other studies related to biofilm analysis using CLSM (Neu and Lawrence, 1999; Strathmann et al., 2002; Lee et al., 2007). Bacterial cells in the fouling layer were stained with Sybr Green I (Molecular Probes, Invitrogen) specific to nucleic acid. Sypro Orange (Molecular Probes, Invitrogen) specific to proteins and Nile Red (Molecular Probes, Invitrogen) specific to lipids were used as well. Various fluorescently-labelled lectins (Con A, GS-IB4, GS-II, HPA, PHA-L, PNA, SBA, and WGA) (Molecular Probes, Invitrogen) specific to polysaccharides were included to the cocktail of probes used. The lectins used were chosen to stain a large range of polysaccharides. After staining, the fouling layer was immediately observed using a CLSM system under a 100× magnification objective. In all cases, the optical section was obtained through a step-wise increase of 1 μm.

2.5. *Quantification of structural parameters*

Each series of CLSM images were input into ISA-2 for the calculation of structural parameters (Beyenal et al., 2004b). The selected parameters to describe changes in the fouling layer were porosity and bio-volume.

3. Results and discussions

3.1. *Membrane performance*

All MBRs performed equally well in terms of their removal efficiencies. Over the three sets of experimental runs, the removal efficiencies, calculated by the chemical oxygen demand, were between 92 and 98% regardless of the operating conditions or time.

Fig. 2 shows the membrane TMP performance under different flux conditions. Fouling profiles of each MBR in all three experimental runs did not deviate significantly. All three experimental runs showed similar results, in which the TMP of MBR_{sup}, increased more rapidly than both MBR_{crit} and MBR_{sub}. The TMP of MBR_{sup} exceeded 30 kPa after 36 h of operation for all three runs. The TMP of MBR_{crit} only exceeded the same value after 72 h of operation, while MBR_{sub} did not exhibit any significant signs of TMP increase over the same time period.

A closer look at the fouling profiles of the three MBRs revealed that MBR_{crit} exhibited a distinct three-stage process. This corresponded closely to the three-stage mechanism map for membrane fouling in MBRs (Zhang et al., 2006). In the proposed map, Stage 1 consisted of a short initial rise in TMP due to conditioning fouling of the membrane; Stage 2 reflected a long term rise in TMP either linearly or exponentially; Stage 3 occurred with a sudden rise in TMP, which is commonly referred to as the TMP jump. Evident from Fig. 2, MBR_{crit} experienced all three stages of membrane fouling, with the first 4 h of operation at Stage 1, the next 50 h at Stage 2, and thereafter Stage 3. However, this stage-wise membrane fouling mechanism was not observed for both MBR_{sub} and MBR_{sup}. From the fouling profiles, MBR_{sup} exhibited only Stage 3 of the fouling process, in which the TMP rise was extremely rapid. Other proposed fouling stages were not detected and this could be attributed to the difference in the flux conditions. At increasingly higher flux conditions, Stage 2 became increasingly short due to rapid membrane fouling. It would not be observed eventually if the operating flux was high enough. Similarly, at low or sub-critical flux conditions, only Stage 2 of fouling was observed, with little increase in TMP which suggested marginal membrane fouling. If given sufficient operating time, and as membrane fouling slowly progressed, MBR_{sub} would also exhibit Stage 3 of the fouling mechanism map. Even with the theoretical fouling mechanism map, it was not possible to sufficiently conclude that the actual fouling mechanism experienced in MBRs, regardless of flux conditions, would progress accordingly.

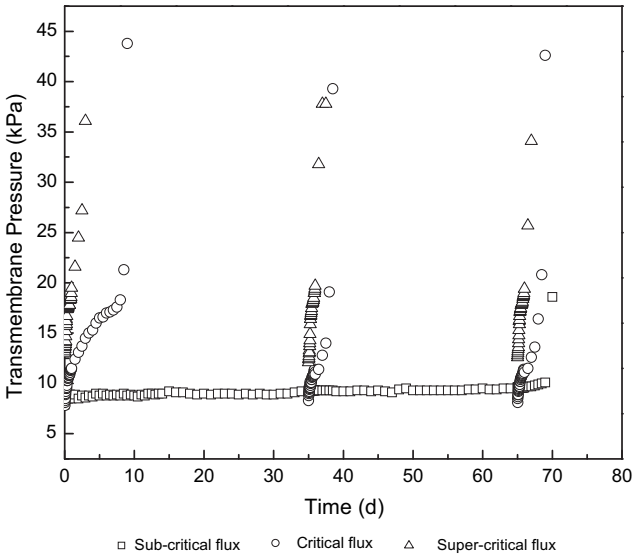

Fig. 2 – MBR performance; TMP against time.

3.2. *Physico-chemical parameters*

Fig. 3 shows the changes in average MLSS concentrations of the three MBRs over time. MLSS concentration fluctuations were related to the HRT of the MBRs. The MLSS concentrations of MBR_{sub} remained constant throughout the study since the MBR had reached steady state, and there were no operational changes. Both MBR_{crit} and MBR_{sup} exhibited increasing MLSS concentrations over time because with an increase in flux, there was a corresponding decrease in the HRT and an increase in both the food-to-mass ratio (F/M) and the volumetric organic loading rate. As such, biomass production in

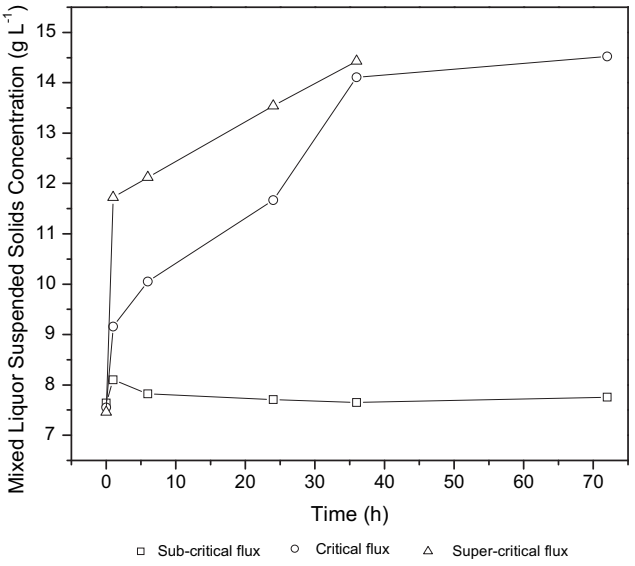

Fig. 3 – Average MLSS concentrations of the three MBRs.

the MBRs operating at higher fluxes increased. Given that the SRT, and thereby the desludging rate, remained the same, the MLSS concentrations in MBR_{crit} and MBR_{sup} naturally increased. With a higher organic loading rate, the MLSS concentration of MBR_{sup} increased more quickly than MBR_{crit}. However, the MLSS concentration of MBR_{crit} remained relatively constant between the 36th h and 72nd h, indicating that it could have reached the limit for further growth. Coincidently, upon reaching the cut-off TMP, the average MLSS concentrations for both MBRs were approximately 14.5 g L^{-1}. As reported in literature, the increase in MLSS concentration resulted in an increase in membrane fouling (Chang and Kim, 2005). This corresponded to the results obtained in which the fouling rate of MBR_{sup} was fastest since it had the highest MLSS concentration at any given time. Yet, using MLSS concentrations as a gauge of fouling propensity is insufficient. Various activated sludge models used in the design of conventional activated sludge systems are deficient for MBRs as they do not account for SMP and EPS concentrations, both which have been reported to be involved in membrane fouling (Jeong et al., 2007).

Fig. 4a–c shows the protein concentrations of the three MBRs over time. Of the protein concentrations quantified in the permeate, SMP and EPS samples, it was found that EPS concentrations were a better indicator of fouling propensity. Due to the characteristics of the synthetic wastewater, in which protein was not present, the presence and detection of protein in the mixed liquor (SMP-protein) could be attributed solely to microbial processes within the MBRs. At the 1st h of operation, protein concentrations in effluent (i.e., permeate), SMP and EPS were consistently lower in MBR_{sub} than those in MBR_{crit} and MBR_{sup}. This relationship changed after the 6th h of operations for effluent and SMP fractions and continued thereafter. Due to the increase in organic loading rate, microorganisms in MBR_{crit} and MBR_{sup} excreted more EPS-protein. Yet, protein concentrations in the permeates of these two MBRs were lower than that of MBR_{sub}. It was also observed that the SMP-protein concentrations in MBR_{crit} and MBR_{sup} were lower than that of MBR_{sub}. This was highly surprising since the MLSS and MLVSS concentrations of the two MBRs were significantly higher than MBR_{sub}. Also, since SMP-protein could be attributed to only microbial processes, an increase in the absolute EPS concentrations should generally lead to a corresponding increase in the absolute SMP concentrations in the bulk solutions, assuming a consistent rate of release of EPS into the bulk solutions by the biomass. Thus based on the lower permeate-protein and SMP-protein concentrations in MBR_{crit} and MBR_{sup}, it was suspected that the excess protein in the two MBRs produced might be found adhered or adsorbed onto the membrane surface. But this must be substantiated by the actual foulants found on the membrane surface, which will be discussed in the later sections. With the presented results thus far, only the EPS concentrations could indicate the possible fouling propensity of the MBRs, rather than the use of SMP concentrations.

A similar conclusion was reached with the carbohydrate concentrations in the MBRs. Fig. 4d–e shows the carbohydrate concentrations in the three MBRs over time. The absolute permeate-carbohydrate concentrations in MBR_{crit} and MBR_{sup} were consistently lower than that found in MBR_{sub}, with a considerable decrease between the 1st and 6th h of the experimental runs. The absolute SMP-carbohydrate concentrations of MBR_{crit} and MBR_{sup} fluctuated around that of MBR_{sub}, which remained relatively constant. Over the experimental runs, MBR_{crit} averaged a higher SMP-carbohydrate concentration than MBR_{sub}, while MBR_{sup} averaged a lower SMP-carbohydrate concentration. Conversely, the EPS-carbohydrate concentrations of the two MBRs were higher than MBR_{sub} at all times. With the use of an easily and rapidly biodegradable substrate (glucose), it was believed that the carbohydrate concentrations detected in the bulk solutions were from microbial processes. Therefore, as with the protein results, it was suspected that the excess carbohydrates observed in the EPS of MBR_{crit} and MBR_{sup} may be found on the membrane surfaces as foulants. This, again, has to be substantiated by the actual foulants detected on the membrane surfaces. With the fluctuations of SMP-carbohydrate concentrations in MBR_{crit} and MBR_{sup}, only the EPS concentrations could accurately serve as a gauge of membrane fouling propensity, similar to that concluded with the protein concentrations.

However, the protein and carbohydrate concentrations observed were unable to indicate which of the two compounds had a greater impact on membrane fouling. Protein-to-carbohydrate (P/C) ratios were used to identify the impact of proteins and carbohydrates on membrane fouling, in relation to each other (Ng et al., 2006). Based on the P/C ratios obtained in the study, it was found that the carbohydrate fraction could have a greater impact on membrane fouling than the protein fraction. Due to the lack of changes in operating conditions, the EPS P/C ratio of MBR_{sub} remained relatively constant at 1.87 ± 0.06. This contrasted with the P/C ratios of MBR_{crit} and MBR_{sup}, which were 1.22 ± 0.08 and 1.19 ± 0.07, respectively, after 24 h of operation. Based on the results, it was concluded that membrane fouling propensity increased as the EPS P/C ratio decreased. This meant that the rate of fouling increased as the EPS-carbohydrate concentrations increased. By the same token, it may be concluded, albeit only preliminarily, that the carbohydrate fraction affected membrane fouling more

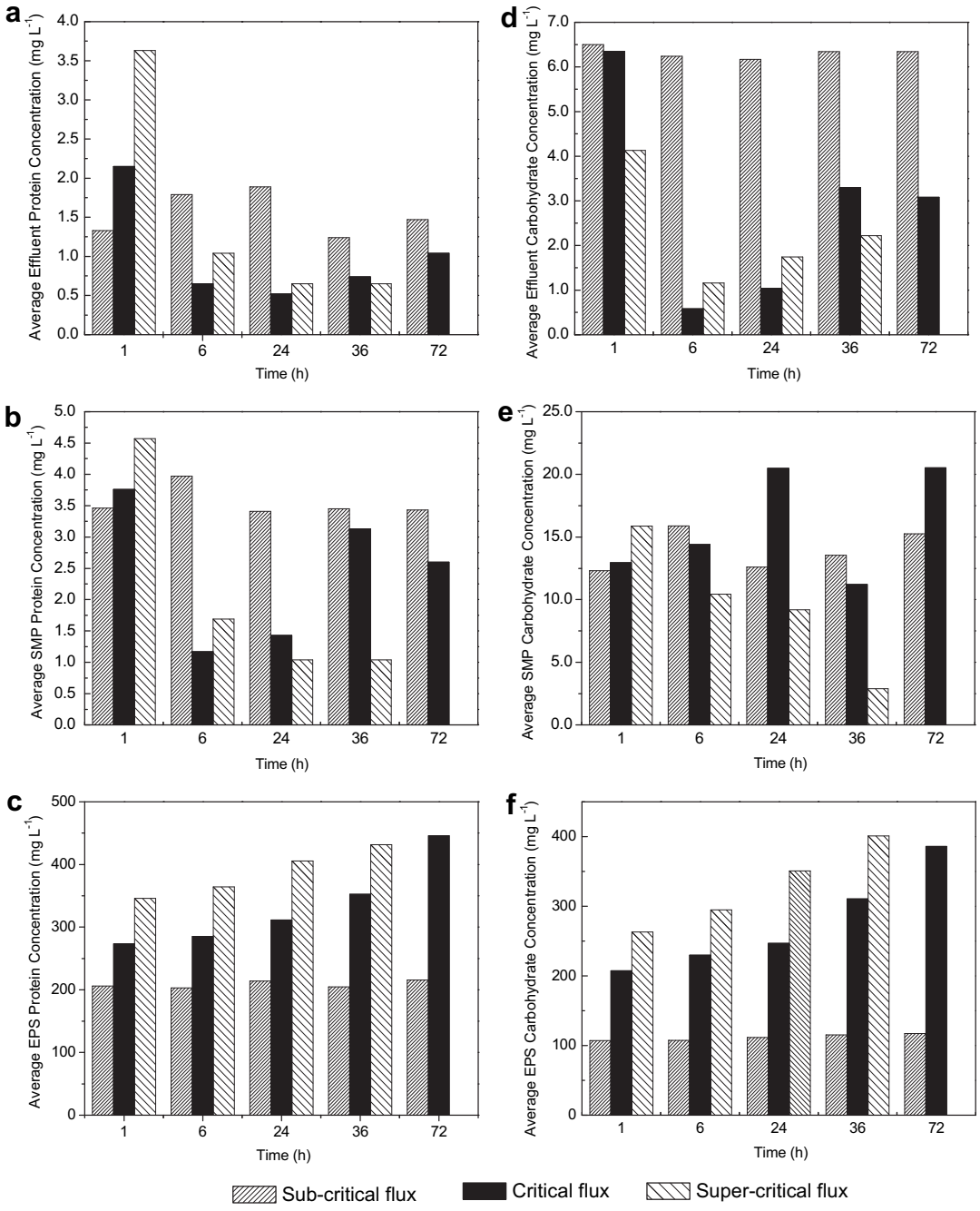

Fig. 4 – Average protein concentrations of (a) permeate, (b) SMP, and (c) EPS. Average carbohydrate concentrations of (d) permeate, (e) SMP, and (f) EPS.

adversely than the protein fraction. However, such conclusions must be substantiated by the actual foulants found on the membrane surface as the carbohydrate fraction in the bulk solution could assimilated by the bacterial cells rather than to be found adsorbed on the membrane surface.

While the use of physico-chemical characteristics to determine possible membrane fouling propensity has generally been accepted due to the relative ease and speed of the tests conducted, it has been also reported that colorimetric methods are insufficient to elucidate membrane fouling in MBRs, and that the characteristics of the organic and microbial by-products (SMP) in the system must be considered (Kimura et al., 2009). Therefore, EEM analyses of the samples could aid in understanding the fouling propensity of the different bulk solutions. Both EEM analyses and that of foulants on the membrane surfaces will be discussed in the next sections.

3.3. *Excitation-emission matrices*

EEM spectra were conducted in triplicate for each run and the results were similar in all measurements. Fig. 5 shows the EEM fluorescence spectra obtained for the permeate, SMP, and EPS

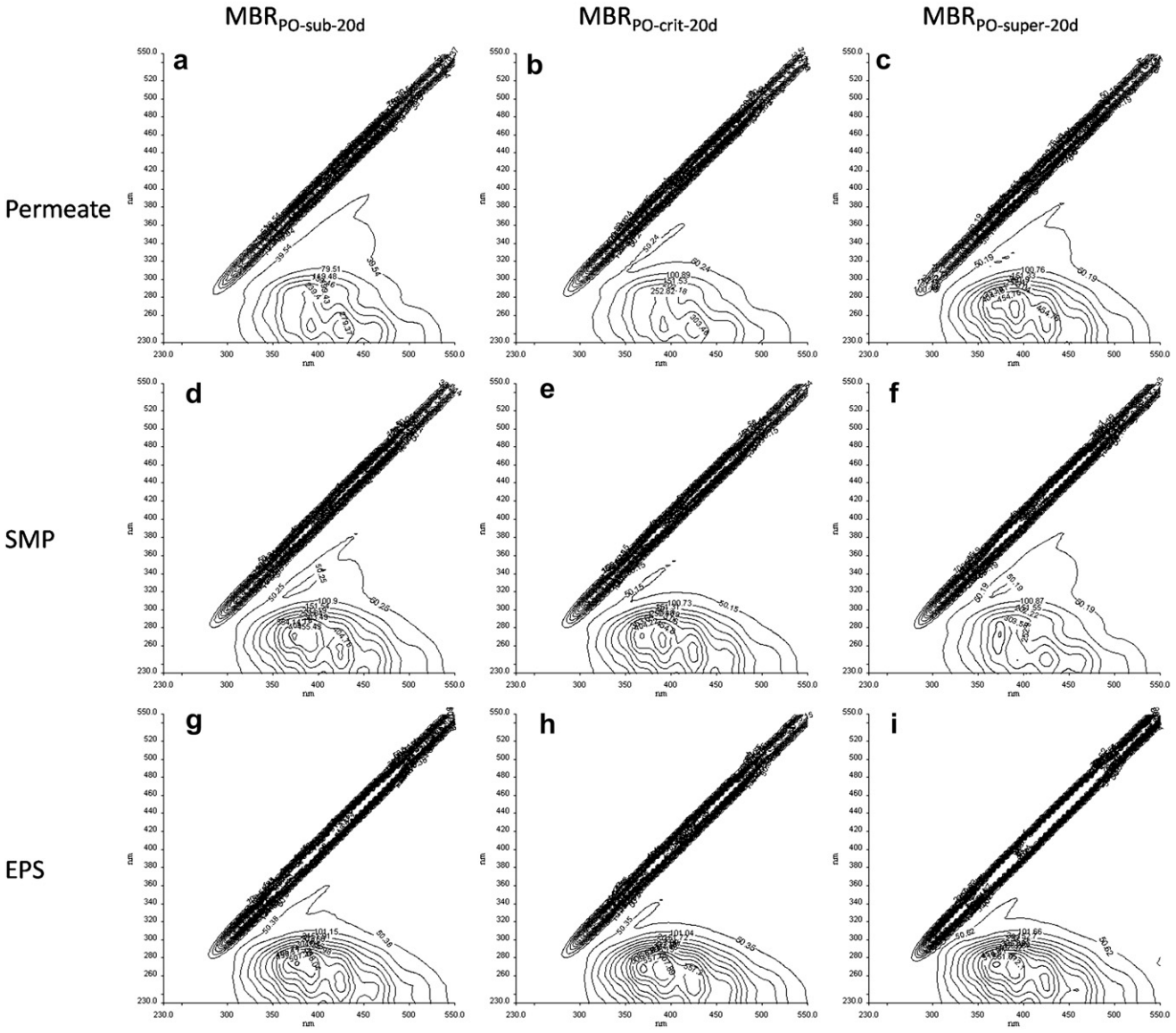

Fig. 5 – Excitation–emission matrices.

samples collected from all MBRs at the end of each experimental run. Shapes of the spectra obtained were significantly different across the MBRs indicating that the characteristics of the samples were altered by HRT. However, it was not possible to determine whether a certain shape or spread of the contour plot would affect membrane fouling more adversely or otherwise. And being a relatively new analytical test for MBRs, there has been insufficient evidence to reach any such conclusions. But, differences between the compounds detected in the permeate, SMP and EPS samples in each MBR showed that the membrane served as a barrier for some of the compounds present in the bulk solution.

The main peaks found in the permeate samples were attributed to fulvic- and humic-like substances, as indicated by the peaks at Ex/Em = 250 nm/390 nm, 250 nm/425 nm, and 270 nm/390 nm. Such peaks were also found in the SMP and EPS samples obtained. However, an additional protein-like substance, likely to be a microbial by-product, was found in SMP and EPS samples, as indicated by the peaks at Ex/Em = 270 nm/370–375 nm (Chen et al., 2003). Such protein-like substances present in the SMP and EPS samples were corroborated by previously published studies (Kimura et al., 2009; Wang et al., 2009). The lack of a protein-like peak in the permeate samples could indicated that such substances could be removed by the filtration process, and may be found adhered to the membrane surface. Since protein was detected in low concentrations in the permeate samples by the colorimetric method, it was likely that such protein-like peaks in the EEM were over-dominated by the other peaks present in the samples, thereby demonstrating a shift in the characteristics of the dominant substances between the SMP and permeate samples. Analysis of the foulants on the membrane surface in another study also showed similar protein-like peaks (Kimura et al., 2009), indicating that protein microbial by-products contributed to membrane fouling, as shown in this study.

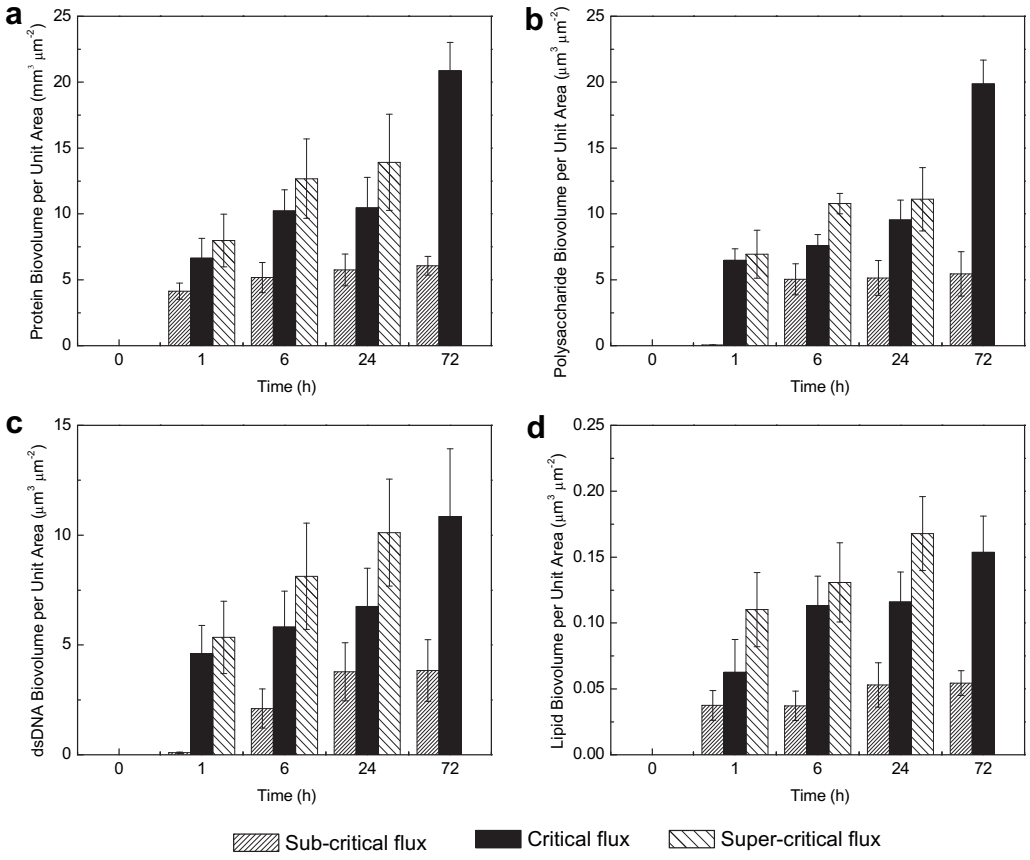

Fig. 6 – Bio-volume of foulants on membrane surface: (a) protein, (b) polysaccharide, (c) cells, and (d) lipid. Y-axis scales of (a) to (d) are different in order to show the differences within each graph. Care has to be taken for the comprehension of the results shown.

While the EEM plots highlighted the distinct shift in the characteristics between the bulk solution (indicated by SMP) and the permeate, showing that protein-like microbial by-products were adhered to the membrane surface, it was incapable of indicating which substance (protein or carbohydrate) caused membrane fouling to a greater extent, or had a greater membrane fouling propensity. CLSM imaging techniques coupled with image analyses could elucidate the relationship between foulants and membrane fouling further.

3.4. *Bio-volume of foulants with time*

Fig. 6 shows changes in bio-volume of the various fouling constituents in each MBR with time. It was found that the most dominant fouling fraction on the membrane surface was protein. In spite of the hydrophilicity of the clean membrane surface, the protein fraction in the bulk solution was the conditioning material. It was likely that hydrophobic–hydrophobic or steric interactions between the protein molecules and the polymeric membrane material lead to the initial adherence (Huisman et al., 2000). The adherence of other fouling constituents was promoted by this protein conditioning layer and this was evident from the 1st-h result of MBR_{sub}. Subsequently, other fouling fractions started to rapidly build up. At the end of 72 h, there were little bio-volume differences in the protein and polysaccharide fractions on the membrane surface. With respect to MBR_{sub}, it could be concluded that the fouling was at Stage 2 of the mechanism map described previously. Fouling in sub-critical flux conditions appeared to go through a biofilm mediated mechanism. After the initial conditioning of the surface, bacterial cells slowly colonised the membrane surface, albeit sparsely. Further membrane fouling occurred through the subsequent development of a biocake on the surface, in which other bacteria were attracted and adhered to by the EPS produced from the existing bacteria on the membrane surface. Some bacteria, protein and polysaccharide were also suspected to be introduced onto the membrane surface via the suction pressure, in which those compounds were forced into close contact with the membrane surface and thereby enhancing the chances of attachment onto the membrane surface.

This non-biofilm bio-organic fouling mechanism via the suction pressure became increasingly apparent as the flux increased and was observed in MBR_{crit} and MBR_{sup}. At each time interval, there were little significant differences in the bio-volume of cells, protein and polysaccharide for MBR_{crit}. It is believed that through increasing the flux in the MBR, membrane fouling materials were brought to the surface faster and more forcefully. This increased attachment of the foulants regardless of the surface conditions of the membrane. Therefore, bio-volumes of the three most

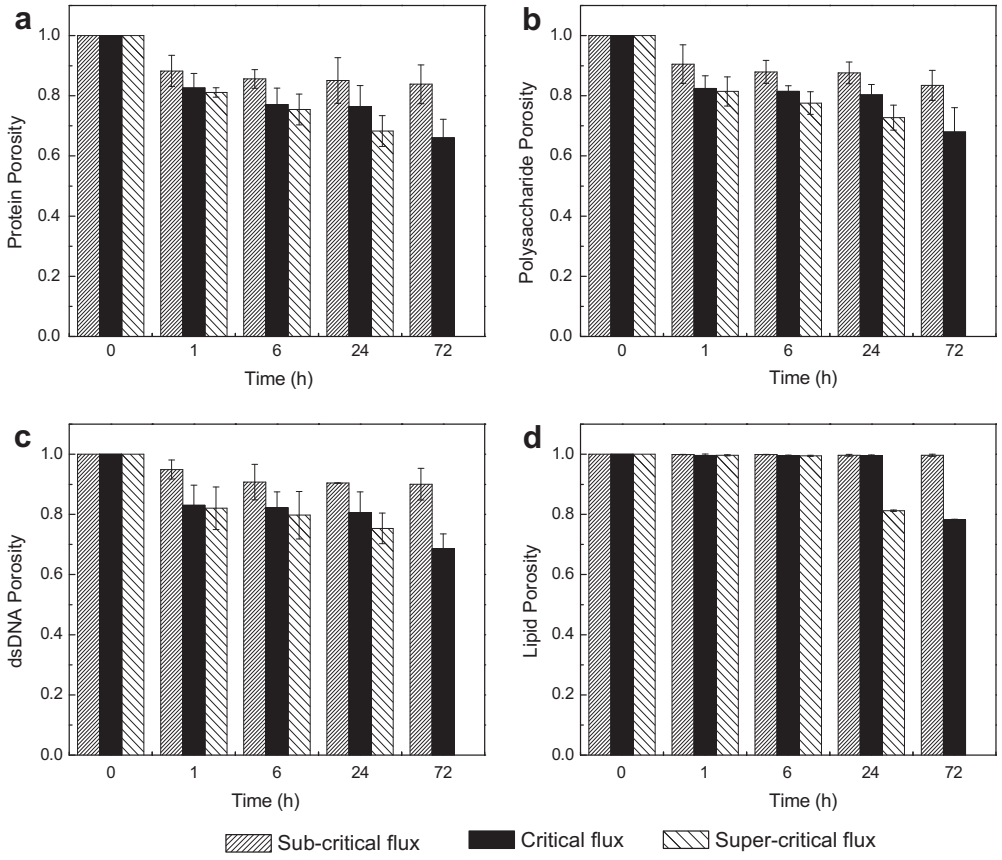

Fig. 7 – Porosity of foulants on membrane surface: (a) protein, (b) polysaccharide, (c) cells, and (d) lipid.

dominant fractions were very similar at each time interval in MBR_{crit}. However, this effect was less pronounced at even higher flux conditions. Protein, which was found as the fraction that adhered most readily to the membrane surface, was the most dominant organic fouling compound but this effect was not through a biofilm developmental mechanism as noticed in MBR_{sub}, as the bio-volumes of the other fouling constituents were significantly high as well. Such results corroborated with the physico-chemical analyses of this study, in which the excess EPS generated may be found on the membrane surface regardless of the lower SMP concentrations in MBR_{crit} and MBR_{sup} compared to those observed in MBR_{sub}, further suggesting EPS as a good indicator of membrane fouling propensity.

When compared to the other fouling constituents, the lipid fraction was insignificant for all MBRs. These lipids observed were simply by-products of the bacterial cells on the membrane surface and appeared to have little effect on membrane fouling.

3.5. *Porosity of foulants with time*

Porosity results corroborated with bio-volume observations. Fig. 7 shows the porosities of the various constituents in each MBR with time. The porosity values were average porosity values of each three-dimensional CLSM series, and were able to accurately reflect the amount of voids within the foulant layer on the membrane surface. The porosities of all fractions decreased with increasing time and flux in all MBRs. These results agreed with with previously conducted studies (Lee et al., 2007; Yun et al., 2006) and were not unexpected since the overall foulant coverage on the membrane surface generally only increased with time. With increased coverage, there would be a corresponding decrease in porosity. Since the thickness of the fouling layer also increased with time and flux, and when the fouling layer became denser with

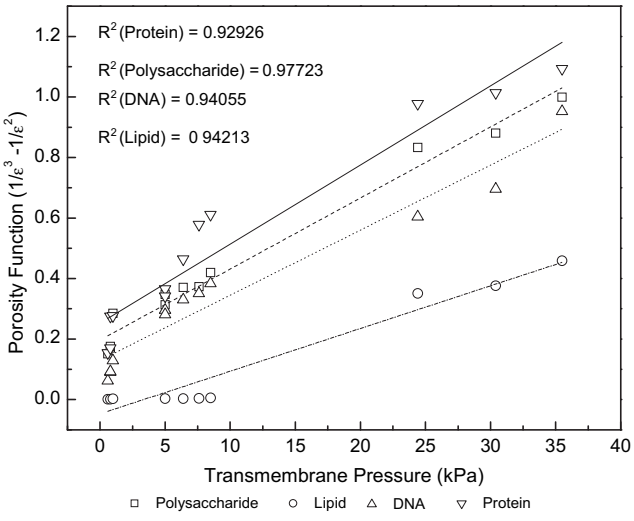

Fig. 8 – Effect of individual foulants on TMP.

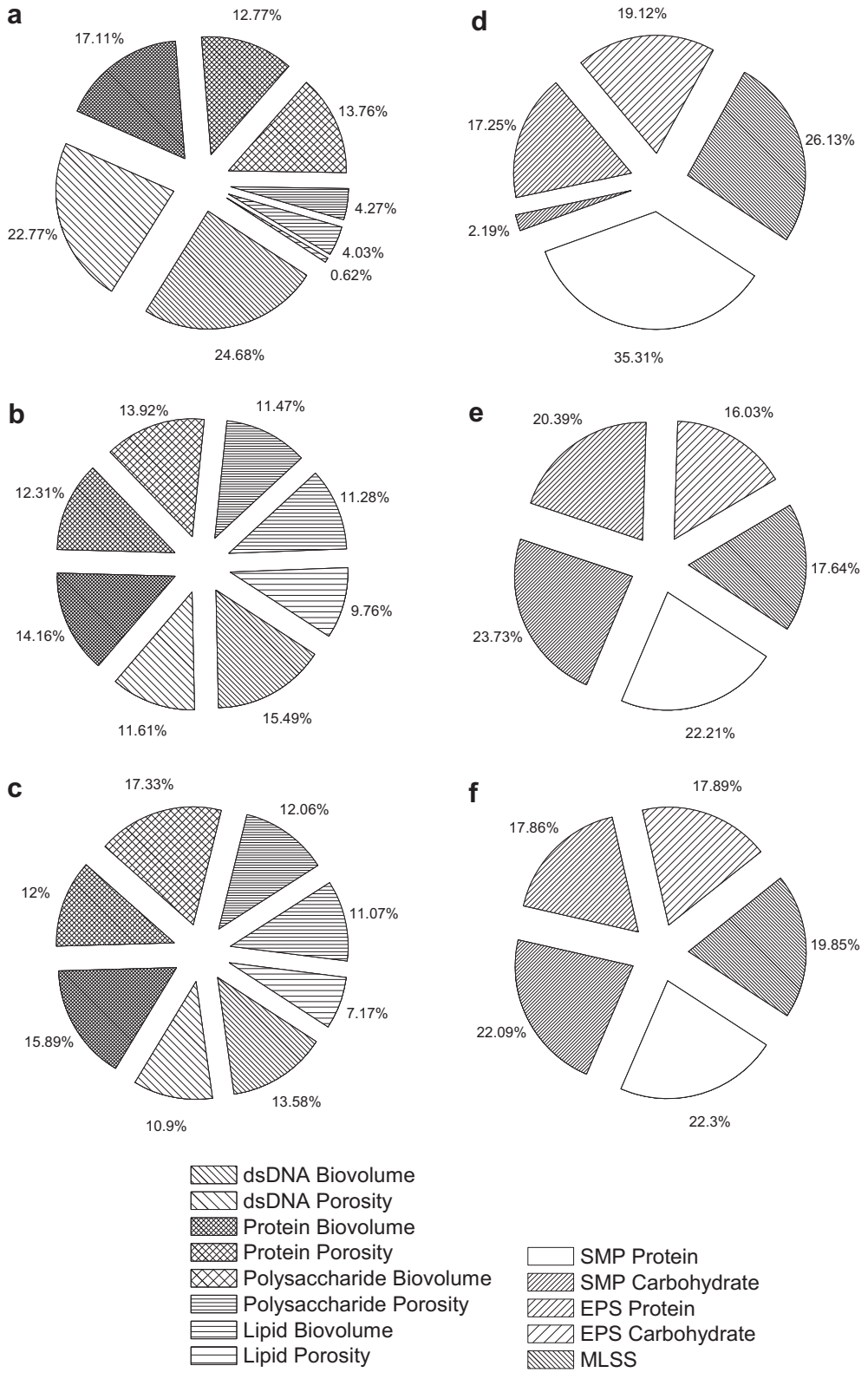

Fig. 9 – Ordered effect figures of (a–c) micro-structural characteristics on TMP of MBRs operated at (a) sub-critical, (b) critical, and (c) super-critical flux conditions; (d–e) physico-chemical parameters on TMP of MBRs operating at (d) sub-critical, (b) critical, and (c) super-critical flux conditions.

increased flux through its compression, the overall average porosity of the three-dimensional fouling layer became lower.

Of the four constituents targeted, the protein fraction had the lowest porosity value for all time intervals, regardless of the MBR. This was followed by the polysaccharide, cells, and lipid fractions. Thus, a comparison of the porosities hinted that the individual effect of each organic foulant was different on membrane fouling. As such, it was believed that the protein fraction was the most important fraction that contributed to the rise in TMP, with the lipid fraction as the least important.

In the cells, protein and polysaccharide fractions, the porosities of MBR_{crit} and MBR_{sup} were found to be significantly different at the same time interval at 95% confidence level, with the exception of a few cases. It must be noted that the cases that were similar reflected similar TMP values for those time intervals. A further comparison of porosities of the individual fouling fractions that registered similar TMP, regardless of the time of operation or MBR, showed that the porosity values were not significantly different at 95% confidence level. This meant that porosity was closely linked to the TMP value. As such, it was suspected that the porosity values had a distinct relationship with TMP.

3.6. *Effect of foulants on membrane fouling*

The relationship between TMP and porosity was obtained from equations developed in early filtration studies (Carmen, 1938; Chudacek and Fane, 1984). The flux of an MBR can be expressed by

$$J = \frac{\mathrm{TMP}}{R_m \eta + R_g \eta} \tag{1}$$

and the gel resistance is given by

$$R_g = \left(\frac{aVC_b}{A}\right) \tag{2}$$

Since the Carmen–Kozeny equation (Carmen, 1938) states that

$$a = \frac{180(1-\varepsilon)}{\rho\left(d_p^2 \varepsilon^3\right)} \tag{3}$$

The gel resistance can be expressed as

$$R_g = \frac{180(1-\varepsilon)}{\rho\left(d_p^2 \varepsilon^3\right)}\left(\frac{aVC_b}{A}\right) \tag{4}$$

The relationship between TMP and porosity can be obtained by combining the equations (1) and (4):

$$\mathrm{TMP} \propto \left(\frac{1}{\varepsilon^3} - \frac{1}{\varepsilon^2}\right) \tag{5}$$

Since it was previously shown that porosity was closely linked to TMP regardless of the MBR or flux conditions, all the porosity values of each constituent were combined into one parameter and TMP as the other variable. The porosity function was then plotted against TMP.

Fig. 8 shows the relationship between TMP and the porosity function. It was seen that the porosity function of all fouling constituents had a strong positive relationship with TMP. The effect of each constituent on the rise in TMP was reflected by the gradient of the lines. It could be concluded that protein had the most significant impact on TMP increase, while lipids had the least effect. This result reinforced the notion that protein was the most important fraction that contributed to membrane fouling in this study. However, this contradicted the results obtained from physico-chemical analyses, in which the carbohydrate fraction in the bulk solution was suspected to contribute to TMP rise to a greater extent. Since the microstructure parameters resulted from foulants adhered directly on the membrane surface, it was believed that these parameters were more accurate in identifying the causes of membrane fouling. Therefore, it may be concluded that the carbohydrates in the bulk solution could have been assimilated by bacteria in the activated sludge. Moreover, Zhang and Bishop (2003) also reported that biofilms utilise carbohydrate compounds faster than proteins, thus resulting in skewed physio-chemical results in which carbohydrates contributed to TMP rise to a greater extent. Fouling control may be mitigated by the removal of protein from the membrane surface and by preventing its adherence to the membrane surface.

The effect of bio-volume might be as equally significant as the porosity since it was shown earlier that fouling mechanisms were vastly different under different flux conditions. A multi-level factorial analysis of the various microstructure parameters on their effect on TMP was thus conducted. Fig. 9a–c shows the ordered effect of the micro-structural parameters. The overall bio-volume effect in MBR_{sub} was approximately 60% of the total impact on TMP. This value decreased to 55 and 58% for MBR_{crit} and MBR_{sup}, respectively. This implied that the importance of volumetric foulant attachment on the membrane surface diminished as the flux increased. Although a greater amount of foulants were found adhered to the membrane surface at higher flux conditions, the voids between the foulants gained prominence in fouling development.

Fig. 9a–c also shows the differences in fouling mechanism under different flux conditions. The total effect of bacteria on membrane fouling in MBR_{sub} was found to be 48%, while the effects of protein, polysaccharide, and lipid were 30, 18, and 4%, respectively. In MBR_{crit}, the effects of bacteria, protein, polysaccharide, and lipid were 28, 26, 25, and 21%, respectively. And in MBR_{sup}, the effects of bacteria, protein, polysaccharide, and lipid were 25, 28, 29, and 18%, respectively. Clearly, the fouling mechanism in each MBR was different with the most significant difference in MBR_{sub}. The effect of bacteria was highest in MBR_{sub} and lowest in MBR_{sup}. This reduction in effect indicated that the presence of bacteria on the membrane surface causing membrane fouling became less important with increased flux. Moreover, the differences between the various fouling fractions within each MBR also became less significant with increased flux. These results reinforced the conclusion that the fouling mechanism moved from one that was biofilm initiated to one that was non-biofilm initiated bio-organic fouling as flux increased. As such, fouling control in MBRs has to be case specific in order to operate at higher fluxes for increased permeate volumes.

One of the easiest methods in fouling control is in MBR operations, where process parameters are chosen such that

membrane fouling is minimised. Fig. 9d–f shows the ordered effect of the process parameters on TMP. In MBR_{sub}, the greatest contributions to membrane fouling were SMP-protein (36%), and MLSS (26%). Since it was found that protein was the conditioning foulant in MBR_{sub}, this fraction on the membrane surface could have resulted from SMP-protein. Also, MBR_{sub} underwent a biofilm initiated fouling mechanism, wherein bacteria (or biomass) were comparatively more important to membrane fouling than other fractions and in other MBRs. Therefore, a high contribution from the MLSS concentration served to enhance the proposed fouling mechanism in MBR_{sub}. In the other two MBRs, differences in effects from the various process parameters became less pronounced as flux increased. This, again, hinted that the two MBRs underwent a bio-organic fouling process. Foulants regardless of type were allowed to come into greater contact with the membrane surface at higher fluxes, thereby increasing the chances of attachment onto the surfaces. In MBR_{crit}, the two most important foulants in the bulk solution were SMP-carbohydrate (24%) and SMP-protein (22%), as were in MBR_{sup}. These indicated that the SMP concentrations of protein and carbohydrate contributed to membrane fouling significantly. These results corroborated with micro-structural parameters, in which protein and polysaccharides increased fouling tendency as flux increased. Therefore, in order to reduce membrane fouling at higher flux conditions, protein and carbohydrate concentrations in the activated sludge have to be reduced. It is proposed that in order to operate an MBR at higher flux conditions, the SRT of the MBR has to be longer such that EPS and SMP productions are reduced, and will not adversely affect the rise in TMP.

4. Conclusions

The initial fouling characteristics of aerobic submerged membrane bioreactors (sMBRs) were analysed under different flux conditions. In order to gain a greater appreciation of micro-structural characteristics of the fouling layer on membrane surfaces in relation to membrane fouling, the organic foulants on the surfaces were observed by CLSM and characterised through ISA-2. With variations in operating flux conditions, the following conclusions were made:

1) Membrane fouling rates increased with higher operating fluxes through increased production of MLSS, and EPS concentrations.
2) EEM plots showed a shift in characteristics between the permeate and bulk solution. Protein peaks were absent in the permeate but were present in the SMP samples. This indicated that protein-like microbial by-products were removed by the membrane and found adhered on the membrane surface.
3) Protein was the conditioning foulant on the membrane surface.
4) Bio-volume of the foulants increased with time and flux, while the porosity correspondingly decreased.
5) Protein had the largest overall effect on the rise in TMP regardless of the flux conditions. The lipid fraction had the least effect.
6) Physico-chemical analyses suggested that the carbohydrate fraction was more important to membrane fouling. This contradicted with the micro-structural results, wherein protein was the overall most important fraction. This showed the limitations of using only physico-chemical parameters to characterise membrane fouling.
7) Fouling mechanisms in MBRs shifted from a biofilm initiated process in MBR_{sub} to a non-biofilm initiated bio-organic fouling process in MBR_{crit} and MBR_{sup}. Therefore, fouling control has to be specific to the individual MBR system.
8) Based on the results obtained in this study, it is recommended to study the viability of MBR operations at suitably long SRT so as to reduce SMP and EPS concentrations in the mixed liquor.
9) Bioaugmentation of the mixed liquor may be possible to reduce membrane fouling. Selection pressure to enhance populations of *Bacillus* and *Pseudomonas* species for their enzymes that digest carbohydrates and proteins might be effective in reducing membrane fouling.

REFERENCES

APHA, AWWA, WEF, 2005. Standard Methods for the Examination for Water and Wastewater, 21st ed. APHA, Washington DC, USA.

Beyenal, H., Donovan, C., Lewandowski, Z., Harkin, G., 2004a. Three-dimensional biofilm structure quantification. Journal of Microbiological Methods 59 (3), 395–413.

Beyenal, H., Lewandowski, Z., Harkin, G., 2004b. Quantifying biofilm structure: facts and fiction. Biofouling 20 (1), 1–23.

Carmen, P.C., 1938. Fundamental principles of industrial filtration. Chemical Engineering Research and Design 16 (a), 168–188.

Chang, S., Judd, S.J., 2002. Air sparging of a submerged MBR for municipal wastewater treatment. Process Biochemistry 37 (8), 915–920.

Chang, I.S., Kim, S.N., 2005. Wastewater treatment using membrane filtration – effect of biosolids concentration on cake resistance. Process Biochemistry 40 (3–4), 1307–1314.

Chen, W., Westerhoff, P., Leenheer, J.A., Booksh, K., 2003. Fluorescence excitation–emission matrix regional integration to quantify spectra for dissolved organic matter. Environmental Science and Technology 37 (24), 5701–5710.

Chudacek, M.W., Fane, A.G., 1984. The dynamics of polarisation in unstirred and stirred ultrafiltration. Journal of Membrane Science 21 (2), 154–160.

Dubois, M., Gilles, K.A., Hamilton, J.M., Rebers, P.A., Smith, F., 1956. Colorimetric method for determination of sugars and related substances. Analytical Chemistry 28 (3), 350–356.

Gander, M., Jefferson, B., Judd, S., 2000. Aerobic MBRs for domestic wastewater treatment: a review with cost considerations. Separation and Purification Technology 18 (2), 119–130.

Huisman, I.H., Prádanos, P., Hernández, A., 2000. The effect of protein–protein and protein–membrane interactions on membrane fouling in ultrafiltration. Journal of Membrane Science 179 (1–2), 79–90.

Jang, N., Ren, X., Kim, G., Ahn, C., Cho, J., Kim, I.S., 2007. Characteristics of soluble microbial products and extracellular polymeric substances in the membrane bioreactor for water reuse. Desalination 202 (1–3), 90–98.

Jeong, T.Y., Cha, G.C., Yoo, I.K., Kim, D.J., 2007. Characteristics of bio-fouling in a submerged MBR. Desalination 207 (1–3), 107–113.

Jin, Y.L., Lee, W.N., Lee, C.H., Chang, I.S., Huang, X., Swaminathan, T., 2006. Effect of DO concentration on biofilm structure and membrane filterability in submerged membrane bioreactor. Water Research 40 (15), 2829–2836.

Kang, I.J., Yoon, S.H., Lee, C.H., 2002. Comparison of the filtration characteristics of organic and inorganic membranes in a membrane-coupled anaerobic bioreactor. Water Research 36 (7), 1803–1813.

Kang, I.J., Lee, C.H., Kim, K.J., 2003. Characteristics of microfiltration membranes in a membrane coupled sequencing batch reactor system. Water Research 37 (5), 1192–1197.

Kim, A.S., Chen, H.Q., Yuan, R., 2006. EPS biofouling in membrane filtration: an analytic modelling study. Journal of Colloid and Interface Science 303 (1), 243–249.

Kimura, K., Naruse, T., Watanabe, Y., 2009. Changes in characteristics of soluble microbial products in membrane bioreactors associated with different solid retention times: relation to membrane fouling. Water Research 43 (4), 1033–1039.

Lee, W.-N., Chang, I.-S., Hwang, B.-K., Park, P.-K., Lee, C.-H., Huang, X., 2007. Changes in biofilm architecture with addition of membrane fouling reducer in a membrane bioreactor. Process Biochemistry 42 (4), 655–661.

Lewandowski, Z., 2004. Biofilms: their structure, activity, and effect on membrane filtration. In: Proceedings of IWA Speciality Conference, vol. 2, pp. 417–431.

Liang, S., Liu, C., Song, L.F., 2007. Soluble microbial products in membrane bioreactor operation: behaviours, characteristics and fouling potential. Water Research 41 (1), 95–101.

Lowry, O.H., Rosebrough, N.J., Farr, A.J., Randall, R.J., 1951. Protein measurement with the folin phenol reagent. Journal of Biological Chemistry 193 (1), 265–275.

Ma, B.C., Lee, Y.N., Park, J.S., Lee, C.H., Chang, I.S., Ahn, T.S., 2006. Correlation between dissolved oxygen concentration, microbial community and membrane permeability in a membrane bioreactor. Process Biochemistry 41 (5), 1165–1172.

Meng, F.G., Yang, F.L., Xiao, J.N., Zhang, H.M., Gong, Z., 2006. A new insight into fouling mechanism during membrane filtration of bulking and normal sludge suspension. Journal of Membrane Science 285 (1–2), 159–165.

Neu, T.R., Lawrence, J.R., 1999. Lectin-binding analysis in biofilm systems. Methods in Enzymology 310, 145–152.

Ng, H.Y., Tan, T.W., Ong, S.L., 2006. Membrane fouling of submerged membrane bioreactors: impact of mean cell residence time and the contributing factors. Environmental Science and Technology 40 (8), 2706–2713.

Nuengjamnong, C., Kweon, J.H., Cho, J., Polprasert, C., Ahn, K.H., 2005. Membrane fouling caused by extracellular polymeric substances during microfiltration process. Desalination 179 (1–3), 117–124.

Psoch, C., Schiewer, S., 2006. Anti-fouling application of air sparging and backflushing for MBR. Journal of Membrane Science 283 (1–2), 273–280.

Strathmann, M., Wingender, J., Flemming, H.C., 2002. Application of fluorescently labelled lectins for the visualisation and biochemical characterisation of polysaccharides in biofilms of *Pseudomonas aeruginosa*. Journal of Microbiological Methods 50 (3), 237–248.

Visvanathan, C., Ben Aim, R., Parameshwaran, K., 2000. Membrane separation bioreactors for wastewater treatment. Critical Reviews in Environmental Science and Technoology 30 (1), 1–48.

Wang, Z., Wu, Z., Tang, S., 2009. Characterisation of dissolved organic matter in a submerged membrane bioreactor by using three-dimensional excitation and emission matrix fluorescence spectroscopy. Water Research 43 (6), 1533–1540.

Yun, M.-A., Yeon, K.-M., Park, J.-S., Lee, C.-H., Chun, J., Lim, D.J., 2006. Characterisation of biofilm structure and its effect on membrane permeability in MBR for dye wastewater treatment. Water Research 40 (1), 45–52.

Zhang, X., Bishop, P.L., 2003. Biodegradability of biofilm extracellular polymeric substances. Chemosphere 50 (1), 63–69.

Zhang, J., Chua, H.C., Zhou, J., Fane, A.G., 2006. Factors affecting the membrane performance in submerged membrane bioreactors. Journal of Membrane Science 284 (1–2), 54–66.